Progress In Electromagnetics Research C, Vol. 119, 1–16, 2022

Redefining of the Radar Cross Section and the Antenna Gain to Make Them Suitable for Surface Wave Propagation

Quentin Herbette[1, 2], Muriel Darces[3, 4, *], Nicolas Bourey[5], Stéphane Saillant[6], Florent Jangal[5], and Marc Hélier[3, 4]

Abstract—This paper deals with a new definition of the Radar Cross Section (RCS) suitable for surface wave propagation in the HF band. Indeed, it can be shown that the classical definition of the RCS is dependent on distance for this kind of propagation. Also, in simulation, with the classical definition, the power estimated on the receivers using the radar equation is inaccurate. This is an issue for the performance assessment of High Frequency Surface Wave Radars. Thanks to the analysis of different wave propagation models, the differences between the space wave propagation and surface wave propagation have been highlighted. The required modifications of the RCS can then be performed. The proposed new definition is explained and justified in the paper and has been successfully applied to the computation of the RCS of naval targets. In addition, the implementation of this normalization term into the radar equation, and conversely the gain, is discussed. It can be observed that the received power, determined with the definitions adjusted to the surface wave propagation, is accurate. The different obtained results are illustrated and commented.

1. INTRODUCTION

For more than two decades, ONERA (The French Aerospace Lab) has been deploying High Frequency Radars. These radars, operating in HF band (i.e., from 3 MHz to 30 MHz), have established themselves as a low cost solution to detect target beyond the line-of-sight. High Frequency Surface Wave Radar (HFSWR) is of particular interest for monitoring the Exclusive Economic Zone (EEZ). These radars are based on the ability of electromagnetic waves to propagate at the surface of the sea, allowing detections up to 216 nautical miles (400 km). HFSWR have been previously integrated in the European Union research framework on Integrated Maritime Surveillance Systems (IMSS) [1].

Considerable research works dedicated to HFSWR are still ongoing. The majority of them are focused on clutter mitigation, oceanography, and antenna radiation pattern optimization. For example, radiation efficiency can be improved by using metamaterial structures, allowing a considerable increase in the surface wave power radiated by the transmitting antennas [2].

In order to forecast the performance of surface wave radars on their future deployment sites, there is an interest in developing a dedicated simulation software. It is then necessary to solve the radar equation or to know the exact scattered fields impressing the receiving antennas. Therefore, such software will require a database of RCS from different representative targets. The usual definition (1) of the RCS is given in [3], and it appears not suitable for surface wave propagation:

$$\sigma = \lim_{R\to\infty} 4\pi R^2 \frac{|E_s|^2}{|E_0|^2} \tag{1}$$

Received 12 November 2021, Accepted 20 January 2022, Scheduled 28 February 2022

* Corresponding author: Muriel Darces (muriel.darces@sorbonne-universite.fr).

[1] CEA CESTA, 33116 Le Barp, France. [2] Was previously with the ONERA-DEMR, 91123 Palaiseau, France. [3] Laboratoire de Génie Electrique et Electronique de Paris, CNRS, Sorbonne Université, 75252 Paris, France. [4] Laboratoire de Génie Electrique et Electronique de Paris, CNRS, Université Paris-Saclay, CentraleSupélec, 91192 Gif-sur-Yvette, France. [5] Direction Générale de l'Armement (DGA), F-75509 Paris, France. [6] DEMR, ONERA, Université Paris Saclay, F-91123 Palaiseau, France.

Indeed, due to surface wave propagation, the incident field E_0 on the target is neither uniform, nor plane. In addition, electromagnetic fields, and especially the E_s field scattered by the target, do not decay inversely with the distance R. A direct outcome is that the power computed with the radar equation using the classical definitions is erroneous. In consequence, a new definition of the RCS is required in order to normalize the global power budget in the simulation. Our approach is mainly based on the analytical formulation of the field radiated by an elementary dipole as proposed by Bannister [4]. Thanks to the electromagnetic simulation software FEKO, it has been possible to validate that our definition is well suited for surface wave propagation. In order to simulate realistic radar scenes, various naval targets have been modelled using 3D modelling software, and their RCSs have been computed, according to that new definition.

In Section 2, it is highlighted, thanks to numerical simulations, that the usual RCS definition is not suitable for surface wave propagation. Also, from simulation, it is possible to show that a significant error is made on the received power using the classical definitions. In Section 3, in order to adjust the definition of the RCS for surface wave propagation, the analysis of different propagation models is provided. In Section 4, the new definition of the RCS is introduced and is compared to the classical one. In Section 5, the results of our RCS formulation, carried on for several naval targets, are discussed. In Section 6, the integration of the new RCS and gain, modified to suit the surface wave propagation within the radar equation, is carried out. Results, as obtained from simulations, demonstrate the benefit of these modified definitions in calculating the received power. Finally, a conclusion is drawn.

2. IRRELEVANT RCS USUAL DEFINITION FOR SURFACE WAVE PROPAGATION

The RCS is a physical quantity that characterizes the target illuminated at a specific frequency but should not depend on the distance between the radar and the target. In free space, the classical definition of the RCS fulfills these requirements. This is achieved through the convergence of the limit in Equation (1) which cancels the dependency of the RCS according to the distance. As anticipated in the introduction, the magnitude of the HF scattered field over the sea does not decay inversely with the distance. This issue is highlighted here using the electromagnetic simulation software FEKO. The MoM (Method of Moment) solver allows the full-wave computation of such a problem. More precisely, the calculation of Sommerfeld's integral complements Green's dyad and gives the contribution of the surface wave in the total electromagnetic field.

The simulation scene is depicted in Fig. 1: the target is a metallic rectangular plate 40 m high and 50 m wide. It has a zero thickness in the x direction. The upper medium is air, characterized by ϵ_0, the vacuum permittivity, and μ_0, the vacuum permeability. The lower medium is the sea, with the usual electrical parameters: $\epsilon_{rr} = 81$ and $\sigma = 5\,\mathrm{S}\cdot\mathrm{m}^{-1}$ and whose relative complex permittivity is $\underline{\epsilon_r}$ with the harmonic time dependence $e^{\mathrm{j}\omega t}$:

$$\underline{\epsilon_r} = \epsilon_{rr} - \mathrm{j}\frac{\sigma}{\omega\epsilon_0} \tag{2}$$

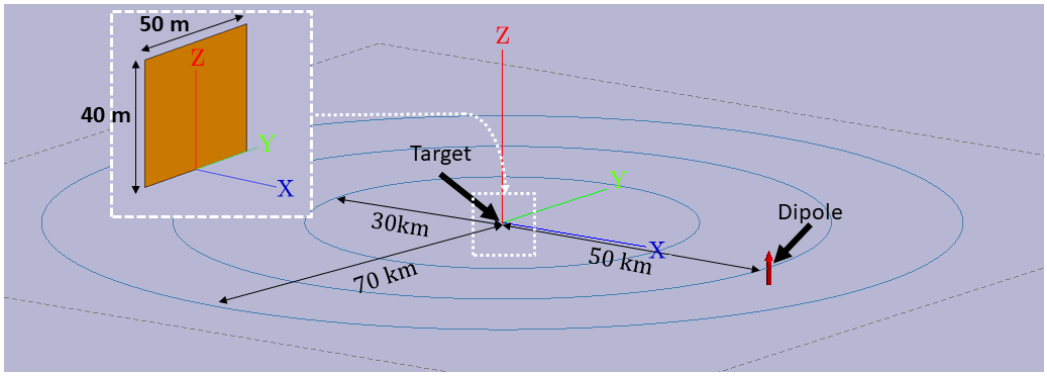

Figure 1. Simulation scene of the scattering of a metallic plate above the sea.

The incident field on the plate is produced by a unitary moment elementary vertical dipole, working at the frequency of 10 MHz, located in the vicinity of the interface ($z = 1$ m), at 50 km from the target, along the x direction.

A first comparison between the electric field computed by FEKO and the field derived by Bannister's formulas [4] has been made in a configuration without the target. Fig. 2 shows the magnitude of the vertical component of the electric field, at altitude $z = 1$ m, as a function of the radial distance from the source. The incident fields thus obtained are identical. Moreover, it can be observed, as it is well known, that the field does not decay inversely with the distance.

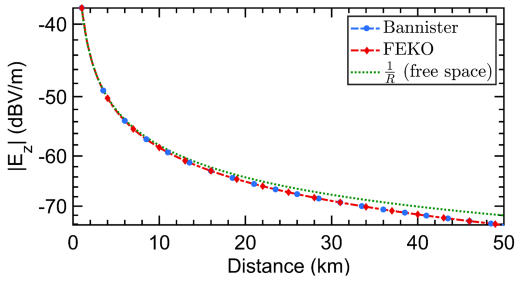

Figure 2. Vertical electric field radiated over the sea at $z = 1$ m by a FEKO dipole (located at zero distance) compared to a Bannister one (at 10 MHz and free space propagation).

Then, the field scattered by the plate is computed, at a height of 1 m, for all azimuthal angles and at distances R of 30, 50, and 70 km. The classical formula (1) is applied to these data in order to compute the bistatic RCS of the target as shown in Fig. 3(a). These results are compared to those obtained in the more usual calculation condition of free-space (Fig. 3(b)).

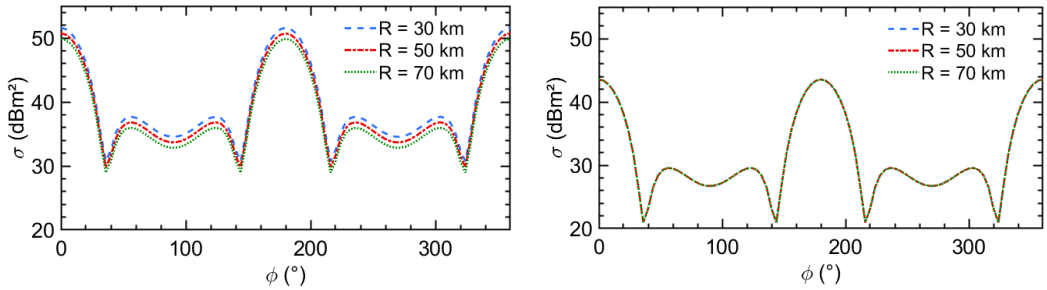

(a) Target over the sea (b) Target in free space

Figure 3. Bistatic RCS σ of the vertical plate, located over the sea, (a) compared to a free space configuration, (b) (at 10 MHz).

It can be seen that the resulting RCS depends on the distance in the case of surface wave propagation and not in the case of free space propagation, as expected. Such a result was predictable because the propagation properties of free-space waves and surface waves differ significantly.

In the previous section, the losses effect on the RCS has been highlighted. The RCS is useful for switching from electromagnetic theory to radar system via the use of the radar equation, and therefore allows the radar to be designed according to the targets to be detected, the observation range and the power involved. In the case of propagation with losses, which is representative of the use of a surface wave radar, the radar equation, in its simplest form is:

$$W_r = \frac{W_t G_t}{4\pi R_A^2} \frac{1}{L_A} \frac{\sigma}{4\pi R_B^2} \frac{1}{L_B} \frac{\lambda^2 G_r}{4\pi} \tag{3}$$

We recall the definition of the following quantities: W_t is the power radiated by the transmitting antenna; W_r is the received power; G_t is the gain of the transmitting antenna; G_r is the gain of the

receiving antenna; σ is the target RCS; R_A and R_B are the transmitter to target and target to receiver distances, respectively; λ is the wavelength used; and L_A and L_B are the propagation losses along the forward and backward paths, respectively. These are due to the interaction between the wave and the sea surface, and are computed [4] relatively to the free space case as follows:

$$L_{A,B} = 20 \log \left(\frac{E_{fs}(R_{A,B})}{E(R_{A,B})} \right) \tag{4}$$

where $E_{fs}(R_{A,B})$ is the magnitude of the field radiated at distance $R_{A,B}$ by the source in free space, and $E(R_{A,B})$ is the magnitude of the field radiated at the same distance by the source above the sea surface.

Gain of the antennas G is closely related to the directivity D and also takes into account the radiation efficiency of the antenna. It is defined, with η being the radiation efficiency of the antenna, as:

$$G(\theta, \varphi) = \eta D(\theta, \varphi) \tag{5}$$

the directivity D is:

$$D = \frac{R^2 S_{\text{rad}}}{\frac{W_{\text{rad}}}{4\pi}} \tag{6}$$

with S_{rad} being the radiated power density and W_{rad} the total power radiated by the transmitter. The interest is now focused on the impact of these terms in the radar equation, especially for the evaluation of the power received by the receiving antenna.

The simulation scene has a transmitter array of three monopoles (separated by a distance of $\lambda/2$ two by two). The target is the container ship, and the receiver is composed of an array of eight monopoles (also separated by a distance of $\lambda/2$ two by two). The simulation is performed for a usual sea ($\varepsilon_{rr} = 81$, $\sigma = 5\,\text{S}\cdot\text{m}^{-1}$) and a frequency of 10 MHz. The simulation scene is shown in Fig. 4. The radar configuration is bistatic with the transmitter located at $R_A = 40$ km from the target and the receiver placed at $R_B = 70$ km. The target is illuminated with $\varphi_i = 0°$ and is observed from an angle $\varphi_s = 15°$.

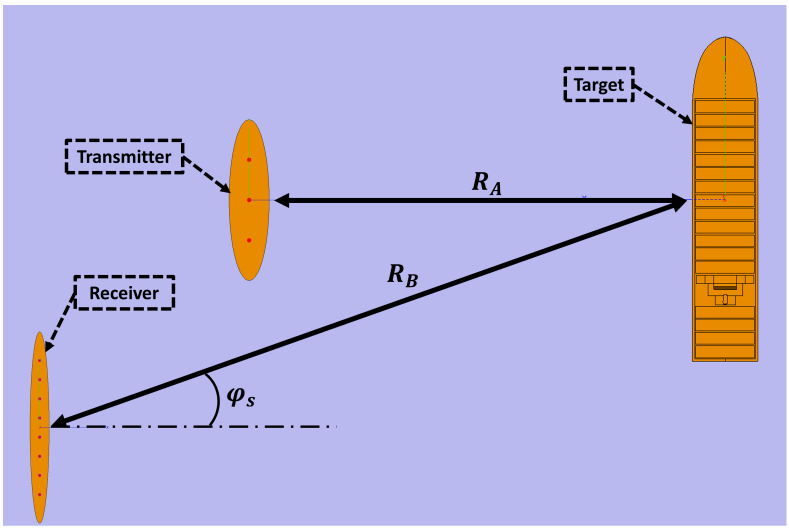

Figure 4. Simulation scene for the application of the radar equation.

The transmitted power W_t is normalized to 1 W. Using FEKO, the incident power density on the target S_i is determined. The power density S_s scattered by the target is evaluated at 70 km from the target at the sea interface. Finally, the received power $W_{R_{FEKO}}$ is obtained by summing the powers on each receiving element. Furthermore, the propagation losses L_A and L_B, with respect to free space, are also obtained by simulation. The values of the different terms are given in Table 1.

Table 1. Terms of the radar equation computed with FEKO.

S_i	$-93.95\,\mathrm{dBW}\cdot\mathrm{m}^{-2}$
L_A	$-4.26\,\mathrm{dB}$
S_s	$-167.33\,\mathrm{dBW}\cdot\mathrm{m}^{-2}$
L_B	$-2.97\,\mathrm{dB}$
$W_{r_{FEKO}}$	$-110.74\,\mathrm{dBm}$

In a first approach, the result given by the classical radar Equation (3) to determine the power on the receiving antennas $W_{r_{cls}}$ is compared to the reference received power $W_{r_{FEKO}}$, computed with FEKO. For this purpose, the transmitter and receiver antenna gains and the RCS are determined using the classical formulations (5) and (1). The transmitter gain G_t is determined (using Equation (6) and assuming a unitary efficiency) at the distance R_A from the source. The RCS σ and receiver gain G_r are estimated (using the same conditions as for G_t) at the distance R_B. The values of the different terms are provided in Table 2.

Table 2. Terms of the radar equation determined using classical equations.

$G_t(\varphi_i = 0°)$	$9.06\,\mathrm{dB}$
$\sigma(\varphi_d = 15°)$	$34.63\,\mathrm{dB}\cdot\mathrm{m}^2$
$G_r(\varphi_d = 15°)$	$11.16\,\mathrm{dB}$
$W_{r_{cls}}$	$-100.59\,\mathrm{dBm}$

As expected, the received power calculated using the classical definitions of gain and RCS does not correspond to the power determined in simulation. The classical method overestimates the received power by about 10 dB. Hence, it is clearly necessary to develop a specific approach. A possible solution is to modify, as much as needed, the definitions of the RCS and gain for surface wave propagation. Therefore, it is first required to study the characteristics of such a propagation mode.

3. VARIOUS SURFACE WAVE PROPAGATION MODELS

3.1. Introduction

At the beginning of the 20th century, Guglielmo Marconi, already considered as a pioneer in radio communication, successfully completed the first transatlantic radio-telegraphy link [5]. At that time, it was not known that the ionosphere could, by means of reflection, allow transmissions far beyond the line-of-sight. It was then assumed that this major scientific achievement was due to a surface wave propagation over the sea. This was the outset for many researches dealing with surface wave propagation at the interface of a conductive medium.

Zenneck demonstrated mathematically, in 1907 [6], that a surface wave can propagate at the interface between two media. However, he did not explain what was the source of these waves. Sommerfeld was the first to demonstrate the possible excitation of a surface wave radiated by a physical source on a conductive half-space [7]. He was able to calculate the expressions of electric and magnetic fields radiated by electric and magnetic dipoles placed arbitrarily over a conductive interface.

In addition, Norton in 1937 significantly simplified Sommerfeld's work in order to make it usable by engineers of his time [8]. Norton's theoretical model is still relevant today as it has been validated by experiments on surface wave propagation.

Despite a large number of propagation models available in the scientific literature, the issue of the unsuitability of the classical RCS in the case of surface wave propagation does not seem to have been addressed yet. To that end, the analysis of different propagation models is necessary in order to

synthesize the main characteristics of surface wave propagation. The interest here is mainly focused on three propagation models. The first one is Bannister's model, based on Norton's work: it analytically separates the field in three components, a direct wave, a ground-reflected wave, and a surface wave, radiated by a dipole placed at an arbitrary height above a plane half-space. The second one is Rotheram's model [9]: this analytical model takes the roundness of the Earth into account as well as an exponential variation of the refractive index of the atmosphere. This model is the one recommended by the International Telecommunication Union (ITU). Finally, the last propagation model available is based on the parabolic wave equation [10]. It allows in particular to consider strong variations of the atmospheric refraction index.

3.2. Bannister's Model

Since our formulation of a new RCS suitable for the surface wave propagation will be primarily based on Bannister's work [4], it has been chosen to describe it precisely. The geometry under consideration is depicted in Fig. 5.

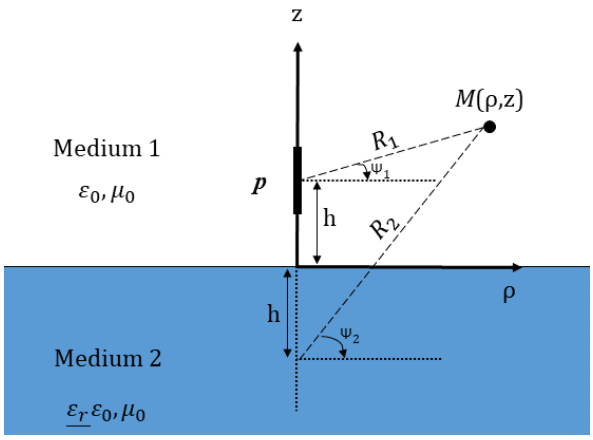

Figure 5. Geometry under consideration.

We are only interested here in the fields radiated by an elementary vertical electric dipole located over the interface, at an altitude h. The impedance of free space is $\eta_0 = 377\,\Omega$; the free-space wave number is k_0; p is the electric-current moment; and the surface impedance normalized to air impedance is Δ:

$$\Delta = \frac{1}{\sqrt{\epsilon_{rr} - \mathrm{j}\dfrac{\sigma}{\omega\epsilon_0}}} \tag{7}$$

The Fresnel reflection coefficient for vertical polarization $\Gamma_{||}$ is defined as:

$$\Gamma_{||} = \frac{\sin\Psi_1 - \Delta_1}{\sin\Psi_1 + \Delta_1} \tag{8}$$

where Δ_1 is:

$$\Delta_1 = \Delta\sqrt{1 - \Delta^2\cos^2\Psi_1} \tag{9}$$

In order to improve the readability of the fields equations, they have been simplified with the assumption that the observation point is located at a large distance from the dipole ($|k_0 R_2| \gg 1$).

The various non-zero fields components, in cylindrical coordinates, are:

$$E_\rho = \frac{\mathrm{j}k_0\eta_0 p}{4\pi}\left(\sin\Psi_1\cos\Psi_1\frac{e^{-\mathrm{j}k_0R_1}}{R_1} + \Gamma_{||}\sin\Psi_2\cos\Psi_2\frac{e^{-\mathrm{j}k_0R_2}}{R_2} - (1-\Gamma_{||})\Delta F(\mathrm{w})\cos\Psi_2\frac{e^{-\mathrm{j}k_0R_2}}{R_2}\right) \tag{10}$$

$$E_z = -\frac{\mathrm{j}k_0\eta_0 p}{4\pi}\left(\cos^2\Psi_1\frac{e^{-\mathrm{j}k_0R_1}}{R_1} + \Gamma_{||}\cos^2\Psi_2\frac{e^{-\mathrm{j}k_0R_2}}{R_2} + (1-\Gamma_{||})F(\mathrm{w})\cos^2\Psi_2\frac{e^{-\mathrm{j}k_0R_2}}{R_2}\right) \quad (11)$$

$$H_\varphi = \frac{\mathrm{j}k_0 p}{4\pi}\left(\cos\Psi_1\frac{e^{-\mathrm{j}k_0R_1}}{R_1} + \Gamma_{||}\cos\Psi_2\frac{e^{-\mathrm{j}k_0R_2}}{R_2} + (1-\Gamma_{||})F(\mathrm{w})\cos\Psi_2\frac{e^{-\mathrm{j}k_0R_2}}{R_2}\right) \quad (12)$$

As can be seen, the fields components are the sum of a direct wave, a ground-reflected wave, characterized by the Fresnel reflection coefficient $\Gamma_{||}$, and a surface wave involving the function $F(\mathrm{w})$. $F(\mathrm{w})$ is the Norton attenuation function and is expressed as:

$$F(\mathrm{w}) = 1 - \sqrt{\pi\mathrm{w}}e^{-\mathrm{w}}\mathrm{erfc}\left(\mathrm{j}\sqrt{\mathrm{w}}\right) \quad (13)$$

where w is the Sommerfeld numerical distance and is defined as:

$$\mathrm{w} = \frac{1}{2}\mathrm{j}k_0R_1\Delta^2\left(1-\Delta^2\right) \quad (14)$$

and where the complementary error function erfc is:

$$\mathrm{erfc}\left(\mathrm{j}\sqrt{\mathrm{w}}\right) = \frac{2}{\sqrt{\pi}}\int_{\mathrm{j}\sqrt{\mathrm{w}}}^{\infty} e^{-z^2}\,\mathrm{d}z \quad (15)$$

It is remarkable that, when the transmitting antenna is located at the interface ($h = 0\,\mathrm{m}$), which is a common scenario for HF radar, the longitudinal to vertical electric field magnitude ratio for $\Psi_1 = \Psi_2 = 0$ is $|\frac{E_\rho}{E_z}| = |\Delta|$.

As an example, for a usual sea and at 10 MHz, $|\Delta| \approx 0.0105$. A low ratio can be observed for the whole HF band, explaining why we generally consider only the vertical field to be of interest in HFSWR.

The study with this propagation model is limited by the validity of the flat Earth model. It has been shown that the corresponding distance limit is [11]:

$$d_c = R_e\left(\frac{\pi}{\lambda_0}R_e\right)^{-\frac{1}{3}} \quad (16)$$

with $R_e = 6371.10^3\,\mathrm{m}$ the radius of the Earth. The analysis carried out here at 10 MHz is therefore restricted to a maximum distance of $d_c = 70\,\mathrm{km}$. The curves below show the variations, normalized at sea level, of the amplitude and the phase of the electric field as a function of the altitude. This comparison is performed for several distances between 30 and 70 km.

Useful information can be deduced from Fig. 6. Firstly, even if the amplitude of the field is not uniform, the amplitude variations as a function of altitude, at a fixed distance, are small, in the order of 10% at 100 m. Secondly, these variations as a function of altitude are almost linear and change not much with distance. Similar conclusions can be drawn for the phase. In order to reinforce these conclusions, particularly at large distances for which flat Earth hypothesis is no longer valid, a similar analysis has been performed with Rotheram's model via the GRWAVE software.

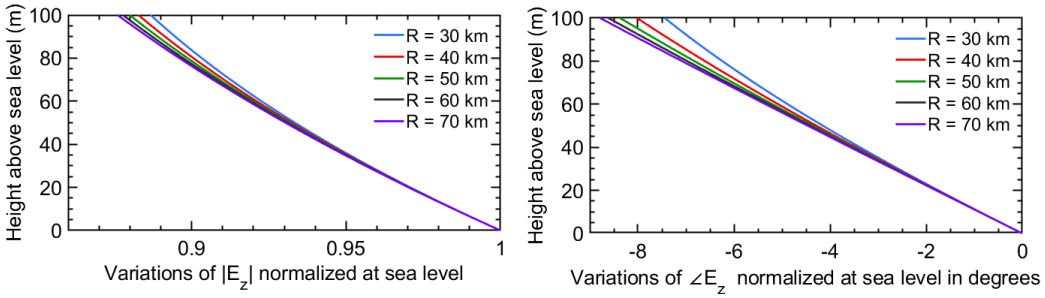

Figure 6. Bannister's model: Variations of E_z (amplitude and phase) at different distances ($f = 10\,\mathrm{MHz}$, sea: $\epsilon_{rr} = 81$ and $\sigma = 5\,\mathrm{S}\cdot\mathrm{m}^{-1}$).

3.3. Rotheram's Model

Rotheram's method is a very comprehensive and analytical model implemented in the GRWAVE [9] software. It allows the calculation of the electric field amplitude at an observation point arbitrarily placed above a round Earth assumed to be homogeneous. This approach can be considered as an extension of Bremmer's work [12]. The latter uses a residue calculation to determine the field radiated by an electric dipole. It should be noted that Bremmer's method, and consequently Rotheram's, as well as the method developed by Norton, have been checked against experimental results [13, 14]. Under the measurement conditions (a terrain with little relief and a low sea state), the comparisons showed that these models, in their respective range of validity, allow an accurate calculation of propagation losses. The behaviour of the surface wave is therefore well modelled.

Since Rotheram's method does not allow the phase of the electric field to be determined, the focus is only on amplitude variations. The analysis is analogous to the one carried out for Norton's model. However, as the range of validity is larger in distance, the analysis is extended up to 200 km.

Significant observations in Fig. 7 are equivalent to those stated with Bannister's model. The variation in field strength with altitude is small, about 10%. Above all, it is interesting to observe that the variation curves converge to a single one from a distance greater than 70 km. The incident wavefront on the target is then substantially the same, whatever the distance is. To take the study further, a similar analysis is carried out with a commonly used numerical propagation model.

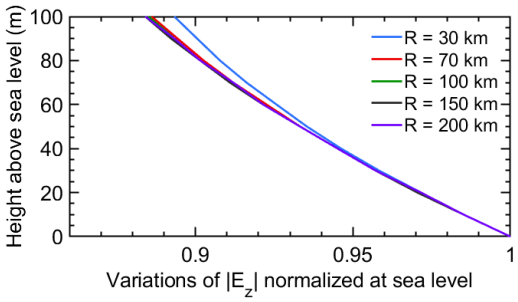

Figure 7. Rotheram's model: Variations of $|E_z|$ at different distances ($f = 10\,\mathrm{MHz}$, sea: $\epsilon_{rr} = 81$ and $\sigma = 5\,\mathrm{S}\cdot\mathrm{m}^{-1}$).

3.4. Parabolic Wave Equation Model

The parabolic equation was introduced in the 1940s by Leontovitch and Fock [15]. Their research dealt with the problem of wave propagation around the Earth. The parabolic equation is so named because a paraxiality hypothesis is applied to derive it. This approach, in view of the initial complexity of the calculation, did not particularly interest the scientific community, and it was not until Tappert introduced the Split-Step Fourier resolution method that it began to be used [16]. It was first applied to the question of underwater sound wave propagation. It proves to be of good efficiency for propagation media with large variations in vertical and horizontal refractive indices. With n the refraction index, the standard 2D parabolic wave equation is:

$$\frac{\partial^2 u}{\partial z^2} - 2\mathrm{j}k_0\frac{\partial u}{\partial r} + k_0^2\left(n^2 - 1\right)u = 0 \tag{17}$$

The literature offers many techniques for solving this equation. The approach used here is a finite element method described by Apaydin [10]. The two-dimensional space is meshed along the abscissa and the ordinate. The discretization steps are respectively δr and δz. The implementation of a Crank-Nicolson method allows a matrix resolution of the system of partial differential equations. A defect of the method used here is that the source is supposed to be Gaussian, which does not correspond to the radiation pattern of a dipole. The necessary modifications are complex and not of great relevance because, at large distances, only the surface wave remains. Consequently, they have not been carried out here.

That propagation model is used for the same frequency and soil parameters as defined in the previous sections. The atmosphere is considered as standard, the horizontal and vertical steps are respectively $\delta r = 100\,\mathrm{m}$ and $\delta z = 10\,\mathrm{m}$.

The analyses previously carried out about the evolution of the amplitude and phase of the electric field as a function of altitude for different distances remain valid with that numerical model, as it can be seen in Fig. 8.

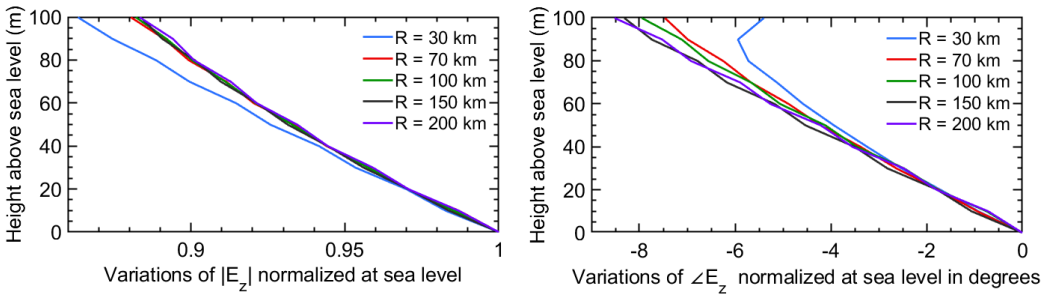

Figure 8. Parabolic Equation: Variations of E_z (amplitude and phase) for different distances ($f = 10\,\mathrm{MHz}$, sea: $\epsilon_{rr} = 81$ and $\sigma = 5\,\mathrm{S}\cdot\mathrm{m}^{-1}$).

These various results form the basis for the reasoning behind the redefinition of the concept of Radar Cross Section applied to surface wave radar. The assumption is that the variations, as a function of distance, of the vertical distribution of electric and magnetic incident fields on the target are negligible. In such a case, the scattering of the target should be independent of the distance. This hypothesis, valid in the band of interest [5–15 MHz], has been extended by looking at the impact of the sea on propagation. The sea state has been taken into account using the method developed by Barrick [17], and the conclusions are the same as for a glassy sea.

4. A RCS DEFINITION SUITABLE FOR SURFACE WAVE PROPAGATION

There are few references in the literature on surface wave Radar Cross Section, that is potentially due to the confidential nature of that topic. Some works dealing with RCS for HFSWR consider a perfect electrically conductive ground [18], which intrinsically does not allow the excitation of a surface wave. Others deal with the question by introducing the notion of apparent RCS [19]. In this case, they associate propagation and RCS in a single quantity σ_a with $\mathfrak{F}$ which accounts for the propagation losses with respect to free space (where the RCS σ_{fs} is defined in free space):

$$\sigma_a = \mathfrak{F}^4 \sigma_{fs} \tag{18}$$

This definition is applied to determine the RCS for a given propagation medium. It requires a propagation calculation to be performed for the different simulation scenes. The concept of apparent RCS loses its meaning as it no longer characterises the target only. However, apparent RCS is very useful for propagation media that are complex to process, for example in the case of scattering from a target behind an island. Our work takes place in the classical framework of target detection with a HFSWR, with a target detected without any obstacle between the radar and the target. The definition of RCS suitable for surface wave propagation called σ_{SW} follows the steps of the definition of the classical RCS. The source of the incident wave is assumed to be close to the ground. The incident power density S_i, related to the vertical field, in cylindrical coordinates, is:

$$S_i = \frac{1}{2} E_{z_i} H^*_{\varphi i} = \frac{1}{2} \frac{|E_{z_i}|^2}{\eta_0} \tag{19}$$

The subscript i stands for incident. As seen in the previous section, the distribution of the field varies according to the altitude. The assumption here is that the field follows the same variation along

the altitude regardless of the distance. It is then possible to express the incident field power density as the arithmetic mean of this density on the target, with h_{target} denoting the height of the target.

$$S_i = \frac{1}{2\eta_0}\frac{1}{h_{target}}\int_0^{h_{target}} |E_{z_i}(z)|^2 dz \tag{20}$$

Denoting σ_{SW} the RCS suitable for the surface wave propagation, the power P scattered by the target is:

$$P = \sigma_{SW} S_i = \frac{1}{2\eta_0}\sigma_{SW}\frac{1}{h_{target}}\int_0^{h_{target}} |E_{z_i}(z)|^2 dz \tag{21}$$

The usual definition of the RCS assumes an omnidirectional diffusion of the field which decays inversely with the distance R. That is not compatible with a propagation over the sea. The scattered field must contain the direct field, the reflected field and the correction term, namely the surface wave. The solution is based on Bannister's radiation formulas. It is then necessary to introduce a function C, which is a compensation function for the field variation with distance. Again, for readability, some higher order terms are neglected because they have a very small influence at large distances from the target. This function is dependent on the frequency, the position of the observation point and the ground parameters and is defined using the functions $\Gamma_{||}$ and $F(\mathrm{w})$, introduced in Section 3.2, as:

$$C(\Gamma_{||}, F(\mathrm{w})) = |1 + \Gamma_{||} + (1 - \Gamma_{||})(F(\mathrm{w}))|^2 \tag{22}$$

In this case, with the subscript s which stands for scattered, the power density S_s, radiated by the target, is:

$$S_s = \frac{1}{2}\frac{|E_{z_s}|^2}{\eta_0} = \frac{P}{4\pi R^2}C(\Gamma_{||}, F(\mathrm{w})) = \frac{\sigma_{SW} S_i}{4\pi R^2}C(\Gamma_{||}, F(\mathrm{w})) \tag{23}$$

$$\sigma_{SW} = \frac{4\pi R^2}{C(\Gamma_{||}, F(\mathrm{w}))}\frac{S_s}{S_i} = 4\pi R^2 \frac{1}{C(\Gamma_{||}, F(\mathrm{w}))}\frac{|E_{z_s}|^2}{\frac{1}{h_{target}}\int_0^{h_{target}} |E_{z_i}(z)|^2 dz} \tag{24}$$

Considering the long-distance scattered field, conventionally noted as a limit, the RCS suitable for surface wave propagation is then:

$$\sigma_{SW} = \lim_{R\to\infty} 4\pi R^2 \frac{1}{C(\Gamma_{||}, F(\mathrm{w}))}\frac{|E_{z_s}|^2}{\frac{1}{h_{target}}\int_0^{h_{target}} |E_{z_i}(z)|^2 dz} \tag{25}$$

The convergence of this new definition can be verified by applying it to the configuration considered in Section 2. As it can be seen in Fig. 9(a), the three curves, when plotting the new RCS σ_{SW} for the three previous distances, are superimposed. It shows the suitability of that new definition to surface wave propagation. For comparison, Fig. 9(b) shows the RCS computed using the classical definition. The new formulation makes it possible to define a quantity independent of distance and representative of the reflectivity of canonical targets. In order to simulate radar scenarios typical of the use of HFSWR, a similar analysis must be performed for quasi-realistic targets.

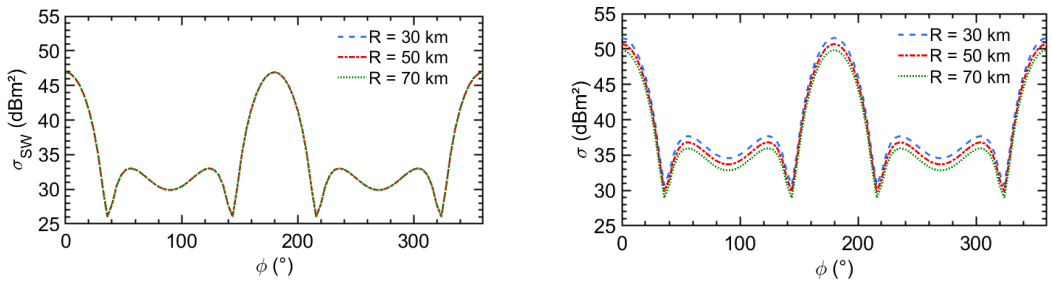

(a) Application of equation (25) (b) Application of equation (1)

Figure 9. Bistatic RCS σ_{SW} of a vertical plate in the case of surface wave propagation, (a) compared to the classical RCS σ, (b) (at 10 MHz).

5. APPLICATION TO VARIOUS NAVAL TARGETS

HF Surface Wave Radars can be employed to cover a variety of threats. This may involve boats of very different sizes, ranging from small boats ($< 15\,\text{m}$) for trafficking activities to very large vessels ($> 200\,\text{m}$), diverging from their shipping routes. The resulting RCS σ_{SW} are illustrated here for two different characteristic targets: a fishing boat dimensioned according to the plans of a fishing vessel common in the Mediterranean and a classic container ship. In the case of the fishing vessel, the interest is focused not only on the convergence of σ_{SW} as a function of distance, but also on the comparison of results for different illuminating sources: dipoles at different distances and a plane wave.

A blueprint and the created 3D model of the fishing vessel can be seen in Fig. 10. Modelling is performed with a free 3D CAD software, which allows the use of NURBS surfaces.

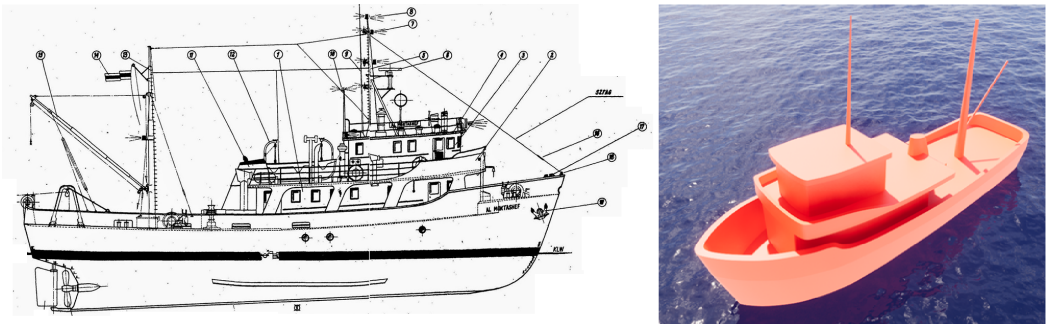

Figure 10. Blueprint and 3D model of the fishing vessel (Blueprint from: http://hobimaketmodel.blogspot.com/).

5.1. Fishing Vessel

The simulation scene can be seen in Fig. 11: the target is a 29.8 m length, 8 m beam, and 13 m air draft fishing boat. The upper medium is air, and the lower medium is the sea. The incident field on the target is generated by an elementary dipole, located in the vicinity of the interface ($z = 1\,\text{m}$), and radiating 50 km away from the target.

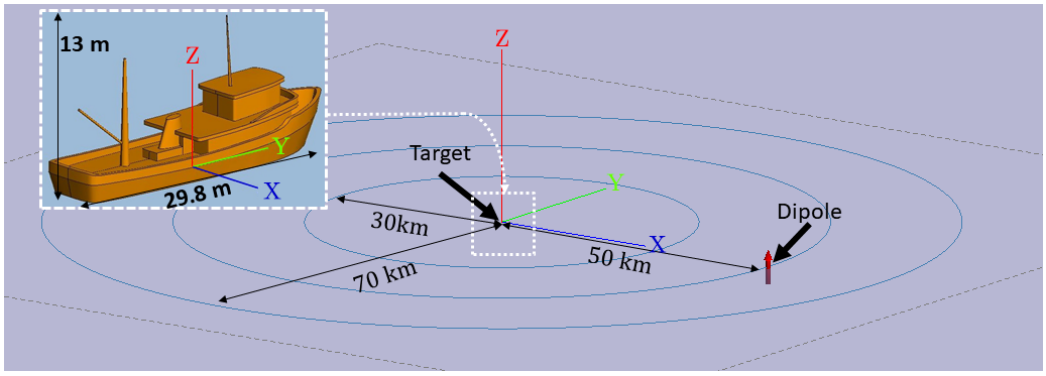

Figure 11. Simulation scene of the scattering of a fishing vessel above the sea.

The scattered field is computed for all azimuthal angles at distances R of 30, 50 and 70 km from the target and at a height of 1 m. The simulation frequency is 10 MHz. Equation (25) is applied to these data in order to compute the bistatic RCS σ_{SW} of the target as shown in Fig. 12(a). For comparison, the RCSs computed using the classical definition in Eq. (1) are depicted in Fig. 12(b). It can be seen that σ_{SW} does not depend on the distance and is anew well suited for surface wave propagation.

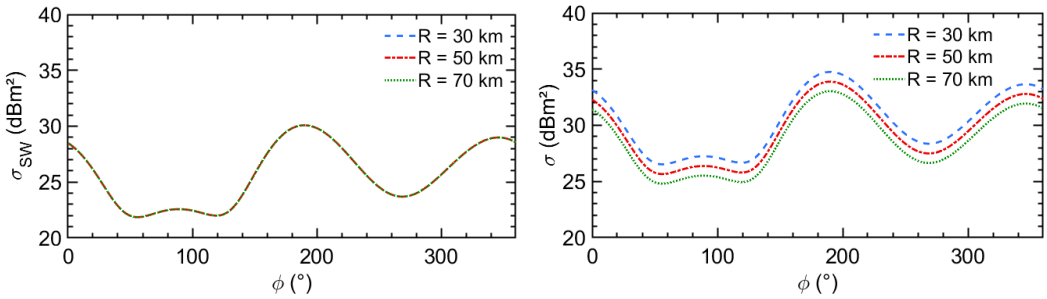

(a) Application of equation (25) (b) Application of equation (1)

Figure 12. Bistatic RCS σ_{SW} of a fishing vessel in the case of surface wave propagation, (a) compared to the classical RCS σ, (b) (at 10 MHz).

The second simulation deals with the comparison of RCS σ_{SW} results for different sources. Indeed, as discussed in Section 3, the vertical distribution of the incident field on the target is critical for the RCS σ_{SW}. The scattered field is calculated here at 50 km for three different incident field sources switched on and off sequentially. These sources are three dipoles placed at 30, 50 and 70 km from the target located alongside the plane $y = 0$. Fig. 12 shows the convergence of the RCS σ_{SW} for one source and several diffraction distances. Fig. 13 shows the convergence of the term for several sources and a single diffraction distance. The resulting curves are exactly alike, which underlines the uniqueness of this new RCS for a given ship at a given frequency.

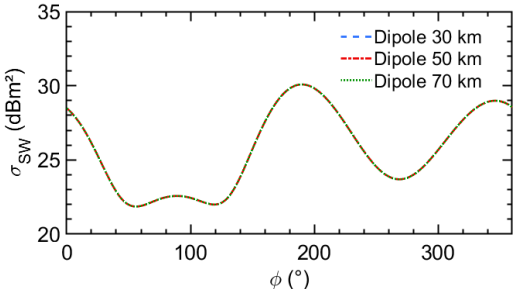

Figure 13. Bistatic RCS σ_{SW} of a fishing vessel illuminated by surface waves emanating from three different location of sources (at 10 MHz).

5.2. Container Ship

With the objective of verifying the expected convergence according to the distance of the RCS σ_{SW} term for large targets, the modelling of a container ship has been carried out. The target is 170 m long, 35 m wide with a vertical clearance of 34 m. The simulation involves an incident field radiated by an elementary dipole. The simulation scene is depicted in Fig. 14. The scattered field is computed for all azimuthal angles at a distance R of 30, 50 and 70 km from the target and at a height of 1 m. The simulation frequency is 10 MHz.

The formula (25) is applied to these data in order to compute the bistatic RCS σ_{SW} of the target. It can be seen in Fig. 15 that the RCS σ_{SW} does not depend on the distance. It is also noteworthy that the variations in RCS depending on the viewing angle are greater than those for the fishing vessel. This can be explained by the quasi-optical behaviour of the incident wave on the target. In fact the wavelength here is electrically small compared to the length of the ship. This latter result confirms that the new definition is well suited to this particular mode of surface wave propagation, even in the case of large targets.

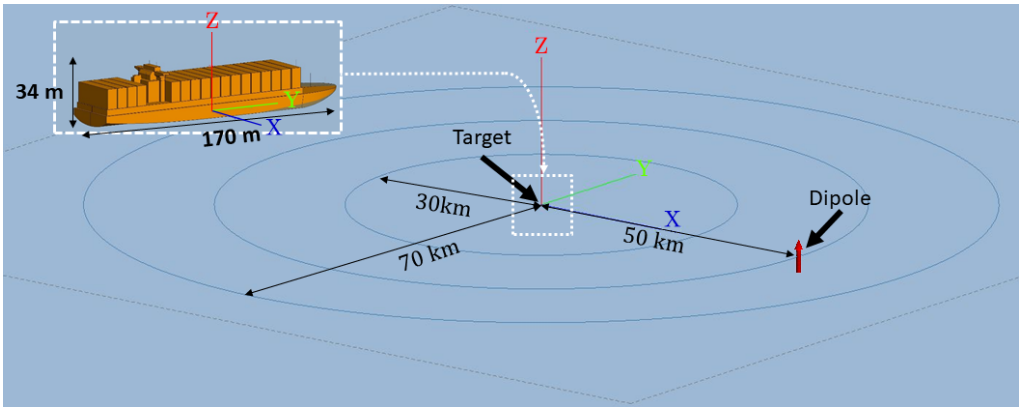

Figure 14. Simulation scene of the scattering of a container ship above the sea.

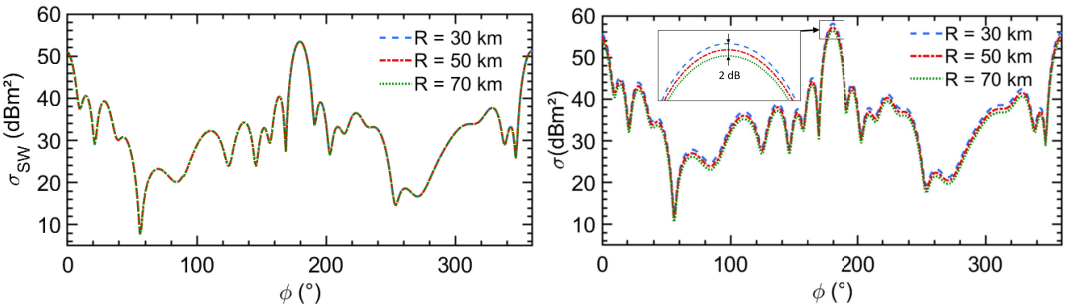

(a) Application of equation (25) (b) Application of equation (1)

Figure 15. Bistatic RCS σ_{SW} of a carrier ship in the case of surface wave propagation, (a) compared to the classical RCS σ, (b) (at 10 MHz).

6. RADAR EQUATION

With the help of different propagation models, significant modifications have been performed to obtain a definition of the RCS suitable for this specific propagation. At the beginning of the paper, it has been announced that it was not possible to determine the power received in simulation with the usual radar equation. It is now necessary to check this assertion in the case of the adjusted RCS definition.

6.1. Gain Definition Suitable for Surface Wave Propagation

In the radar equation, the RCS is not the only term to be defined using assumptions about field propagation. Indeed, Equation (3) involves directivity D, through the gain G of the antennas. In the same way as the RCS, one can question the application of the classical definition of gain for surface wave propagation. For this, we can again investigate the dependency of the gain on the distance. In this part, an array of 3 monopoles in transmission is considered. The main lobe is centered at $\vartheta = 90°$ and $\varphi = 0°$. The system is matched for operation at 10 MHz, and Fig. 16 depicts the antennas used.

Before checking the applicability of the classical definition of gain, the formulas adjusted to surface wave propagation for directivity and gain are introduced. The modification to be made, in order to take into account the surface wave properties, deals with the directivity D. In Equation (6), the squared distance corresponds well to the distance evolution of the power density radiated by the antenna for a classical free space propagation. For surface wave propagation, the directivity D_{SW} is defined using the

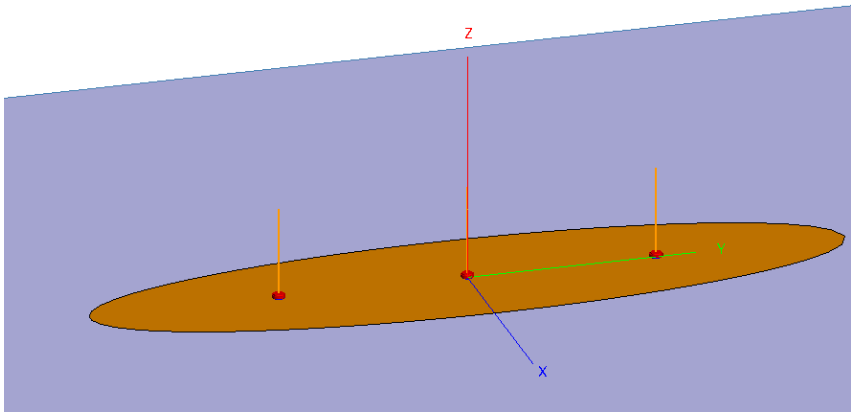

Figure 16. 3D representation of the 3 monopoles antenna array in FEKO.

compensation coefficient $C(\Gamma_{||}, F(\mathrm{w}))$:

$$D_{SW} = \frac{\dfrac{R^2 S_{\mathrm{rad}}}{C(\Gamma_{||}, F(\mathrm{w}))}}{\dfrac{W_{\mathrm{rad}}}{4\pi}} \tag{26}$$

It follows a new expression of the gain G_{SW} of the antenna, given by:

$$G_{SW}(\theta, \varphi) = \eta D_{SW}(\theta, \varphi) \tag{27}$$

Equations (5) and (27) are applied to the obtained simulation data on the monopoles array. The results are presented in Fig. 17. The good convergence of the gain term G_{SW}, modified for surface wave propagation, can be observed. On the contrary, the classical gain G term does not converge as expected and depends on distance.

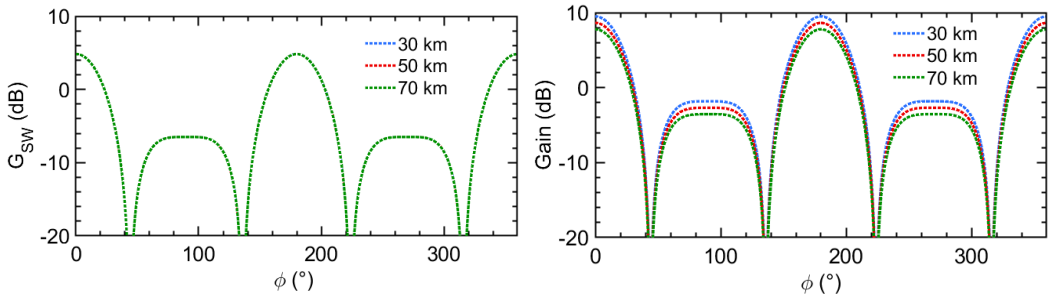

(a) Application of equation (27) (b) Application of equation (5)

Figure 17. Gain G_{SW} of an array of 3 monopoles in the case of surface wave propagation, (a) compared to the classical gain G, (b) (at 10 MHz).

6.2. Simulation and Application to the Radar Equation

After adjusting the gain and the RCS for surface wave propagation, the interest is focussed now on the impact of these terms in the radar equation, especially for the evaluation of the power received by the receiving antenna. The new radar equation considered for the following simulations and applications is the following:

$$W_{r_{SW}} = \frac{W_t G_{t_{SW}}}{4\pi R_A^2} \frac{1}{L_A} \frac{\sigma_{SW}}{4\pi R_B^2} \frac{1}{L_B} \frac{\lambda^2 G_{r_{SW}}}{4\pi} \tag{28}$$

where W_t is the power radiated by the transmitting antenna; $W_{r_{SW}}$ is the received power after application of the definitions tuned for surface wave propagation; $G_{t_{SW}}$ is the transmitting gain; $G_{r_{SW}}$ is the receiver gain; σ_{SW} is the target RCS; R_A and R_B are the transmitter to target and target to receiver distances, respectively; λ is the wavelength; L_A and L_B are the propagation losses respectively for the path between the transmitter and the target and between the target and the receiver.

The simulation scene and its characteristics are shown in Fig. 4, in Section 2. The formulas adjusted to surface wave propagation for gain G_{SW} (Equation (27) assuming antennas with unitary efficiency) and RCS σ_{SW} (Equation (25)) are applied to determine the received power $W_{r_{SW}}$. The different terms, and their values, are summarized in Table 3. It appears that the calculation of the received power ($W_{r_{sw}} = -110.84\,\text{dBm}$) corresponds well to the power obtained in simulation with the FEKO software ($W_{r_{FEKO}} = -110.74\,\text{dBm}$).

Table 3. Factors of the radar equation determined with definitions appropriate for surface wave propagation.

$G_{t_{SW}}(\varphi_i = 0°)$	$4.83\,\text{dB}$
$\sigma_{SW}(\varphi_d = 15°)$	$31.55\,\text{dB}\cdot\text{m}^2$
$G_{r_{SW}}(\varphi_d = 15°)$	$8.21\,\text{dB}$
$W_{r_{SW}}$	$-110.84\,\text{dBm}$

7. CONCLUSION

In this paper, it has been shown that the usual free space definition of the Radar Cross Section and the antenna gain are not suitable in the case of a surface wave propagation, as they are not independent of the distance. Thanks to the study of three analytical and numerical models, an analysis of the surface wave propagation has been performed. Using Bannister's equations set, we have proposed a new definition of the RCS suitable for the surface wave propagation and independent of the observation distance. RCS variations of two distinct ships have been computed and discussed. They confirm the relevance of the new definition of the RCS in the case of surface wave propagation. The interest was then focused on the implementation of this term in the radar equation. For this, it was required to also adjust the definition of the gain to the surface wave propagation using the same approach. It could then be observed that using the two adjusted definitions, the calculated received power corresponds well to the one determined in simulation. In the future, comparisons with measurements undertaken with previous and new prototype of surface wave radars developed by ONERA will be carried out.

ACKNOWLEDGMENT

AID (French Ministry of Defence) is thanked for its contractual support to this work.

REFERENCES

1. Jangal, F. and M. Menelle, "French HFSWR contribution to the European integrated maritime surveillance system I2C," *IET International Radar Conference*, Vol. 2015, 1–5, October 2015.
2. Bourey, N., F. Jangal, M. Darces, and M. Hélier, "Enhancing field strength in HF propagation by using a transition between a metamaterial and the sea," *2013 7th European Conference on Antennas and Propagation (EuCAP)*, 2680–2684, April 2013.
3. Knott, E. F., J. F. Shaeffer, and M. T. Tuley, *Radar Cross Section*, IET Digital Library, January 2004.
4. Bannister, P. R., "New formulas that extend Norton's farfield elementary dipole equations to the quasi-nearfield range," Technical Report NUSC-TR-6883, NAVAL UNDERWATER SYSTEMS CENTER NEW LONDON CT, January 1984.

5. Ratcliffe, J. A., "Scientists' reactions to Marconi's transatlantic radio experiment," *Proceedings of the Institution of Electrical Engineers*, Vol. 121, No. 9, 1033–1039, September 1974.
6. Zenneck, J., "Über die Fortp anzung ebener elektromagnetischer Wellen längs einer ebenen Leiterfläche und ihre Beziehung zur drahtlosen Telegraphie," *Annalen der Physik*, Vol. 328, No. 10, 846–866, 1907.
7. Sommerfeld, A., "Über die Ausbreitung der Wellen in der drahtlosen Telegraphie," *Annalen der Physik*, Vol. 333, No. 4, 665–736, 1909.
8. Norton, K. A., "The Propagation of Radio Waves over the Surface of the Earth and in the Upper Atmosphere," *Proceedings of the Institute of Radio Engineers*, Vol. 25, No. 9, 1203–1236, September 1937.
9. Rotheram, S., "Ground-wave propagation. Part 2: Theory for medium and long distances and reference propagation curves," *IEE Proceedings F — Communications, Radar and Signal Processing*, Vol. 128, No. 5, 285–295, October 1981.
10. Apaydin, G. and L. Sevgi, *Radio Wave Propagation and Parabolic Equation Modeling*, Wiley, October 2017, ISBN: 978-1-119-43211-1.
11. Houdzoumis, V. A., "Two modes of wave propagation manifested in vertical electric dipole radiation over a sphere," *Radio Science*, Vol. 35, No. 1, 19–29, January 2000.
12. Bremmer, H., "Applications of operational calculus to ground-wave propagation, particularly for long waves," *IRE Transactions on Antennas and Propagation*, Vol. 6, No. 3, 267–272, July 1958.
13. Bellec, M., S. Palud, P. Y. Jezequel, S. Avrillon, F. Colombel, and Ph. Pouliguen, "Measurements of surface waves radiated by a vertically polarized antenna over planar seawater at 5 MHz comparison to planar Earth models," *2014 IEEE Radar Conference*, 0245–0250, May 2014, ISSN: 2375-5318.
14. Bellec, M., P. Y. Jezequel, S. Palud, F. Colombel, S. Avrillon, and P. Pouliguen, "Measurements process of vertically polarized electromagnetic surface-waves over a calm sea in the HF band over a spherical earth," *2015 9th European Conference on Antennas and Propagation (EuCAP)*, 1–5, April 2015, ISSN: 2164-3342.
15. Leontovich, M. A and V. A. Fock, "Solution of propagation of electromagnetic waves along the Earth's surface by the method of parabolic equations," *Journal of Physics*, Vol. 10, 13–23, 1946.
16. Tappert, F. D., "The parabolic approximation method," J. B. Keller and J. S. Papadakis, eds., Wave Propagation and Underwater Acoustics, *Lecture Notes in Physics*, 224–287, Springer Berlin Heidelberg, Berlin, Heidelberg, 1977.
17. Barrick, D. E., "Theory of HF and VHF propagation across the Rough Sea, 1, the effective surface impedance for a slightly rough highly conducting medium at grazing incidence," *Radio Science*, Vol. 6, No. 5, 517–526, 1971, eprint: https://agupubs.onlinelibrary.wiley.com/doi/pdf/10.1029/RS006i005p00517.
18. Podilchak, S. K., H. Leong, R. Solomon, and Y. M. M. Antar, "Radar cross-section modeling of marine vessels in practical oceanic environments for high-frequency surface-wave radar," *2009 IEEE Radar Conference*, 1–6, May 2009, ISSN: 2375-5318.
19. Fabbro, V., P. Combes, and N. Guillet, "Apparent radar cross section of a large target illuminated by a surface wave above the sea," *Progress In Electromagnetics Research*, Vol. 50, 41–60, 2005.